CHAPTER V

VERTICAL TWO-PHASE FLOW REGIMES AND PRESSURE GRADIENTS UNDER THE INFLUENCE OF BENZALKONIUM CHLORIDE SURFACTANTS

Supachai Chootongchai[a], Anuvat Sirivat[a,*],

James O. Wilkes[b]

[a]*The Petroleum and Petrochemical College, Chulalongkorn University, Bangkok 10330, THAILAND*

[b]*Department of Chemical Engineering, The University of Michigan, Ann Arbor, MI* 48109-2136, *U.S.A*

5.1 Abstract

The effect of surfactant additive on the two-phase gas/liquid flows regimes, pressure gradients, bubble sizes and velocities was investigated. Experiment was carried out in a vertical transparent tube with inner diameters of 19 mm and the length of 3 m. Water, octylbenzyldimethylammonium chloride solutions (C_8H_{17}-$C_9H_{13}NCl$) and hexadecylbenzyldimethylammonium chloride solution ($C_{16}H_{33}$-$C_9H_{13}NCl$) were used as the working fluids. Adding the surfactant lowers the air critical Reynolds numbers for the bubble-slug flow and the slug flow transitions. The friction factors or the dimensionless pressure gradients of pure water and surfactants are distinctively different depending on the flow regime, the bubble/slug size, the Eotvos number, and property parameter. The normalized bubble and the slug dimension of pure water are greater than those of (C_8H_{17}-$C_9H_{13}NCl$) solution and ($C_{16}H_{33}$-$C_9H_{13}NCl$) solution at any Re_{air},, due to the surface tension effect. The

corresponding normalized bubble and slug velocities of pure water are lower than those of (C_8H_{17}-$C_9H_{13}NCl$) solution and ($C_{16}H_{33}$-$C_9H_{13}NCl$) solution.

Key-words: Fluid mechanics, Surfactant, Pressure gradients, Bubble/slug sizes, Bubble/slug velocity, Flow regimes

*Corresponding author: email anuvat.s@chula.ac.th, Ph: 662 218 4131, Fax: 662 611 7221

5.2 Introduction

Two-phase gas-liquid flow in vertical tube with the addition of a surfactant has been well studied because of the reduced pressure drop and the potential energy saving. Typically for a two-phase flow, there are mainly four flow regimes as dictated by variation in the gas and liquid flow rates. The flow regimes are the bubble, the slug, the annular, and the mist regimes. Characteristics of the flow regimes depend on several factors: the individual magnitudes of the liquid and gas flow rates; the physical properties of liquid and gas, such as density, viscosity, surface tension; and chemical structure. Each flow regime can influence, at different degrees, the heat transfer rate, the momentum transfer, the energy loss, energy exchange rate, and the pressure gradient.

The behavior of a single gas bubble released in a column of liquid within in a vertical tube depends primarily on the size of the bubble. When the bubble is quite small, it remains spherical and rises along a vertical rectilinear path. Larger bubbles become ellipsoidal or irregularly shaped and tend to rise along helical or zigzag paths. With increasing gas flow rate, large cap-shaped bubbles are formed by collisions. When the diameter of the bubbles is nearly the same as the tube diameter, it is the initiation of the slug flow. The churn flow, a transition between the slug and annular regimes, is highly disturbed and has large waves flowing up the channel, interspersed with regions of falling liquid films. In the annular flow, part of it is the liquid film and the rest is dispersed in the gas core in the form of fine droplets. With increasing gas flow rate, the liquid film will be thinner while the number of droplets increases. The mist flow starts when the liquid film is removed from the wall.

Detailed characteristics and measuring methodology of various flow regimes of the two-phase liquid and gas flow can be found from the previous works of Lockhart and Martinelli (1949), Davies and Taylor (1950), Nicklin (1962), Wallis (1969), Sylvester (1987) and Wilkes (1999).

Kawaguchi *et al.* (2002) studied on drag-reducing channel flow with cationic surfactant additives. The surfactant additives suppressed violent vortex motions near the wall.

Usui *et al.* (2004) studied the surfactant drag reduction caused by a cationic surfactant with excess addition of counter-ions. The optimum molar ratio to give a good drag reduction was (surfactant):(counter-ion) = 1:1.5. With further increase in the counter-ion concentration, the apparent viscosity level decreased and the shear thinning behavior was lost, whereas the high drag reduction effectiveness was still retained. The micelle structure could be varied depending on the counter-ion molar ratio, and the modifed structure was also effective for the turbulent drag reduction observed.

Zhang *et al.* (2005) investigated the functional groups on the polar heads of cationic surfactants. Increasing the head group size decreased drag reduction at high temperatures.

Rosso *et al.* (2006) studied the effects of interfacial surfactant contamination on bubble gas transfer. Surface active agents depress gas transfer at gas-liquid interfaces. The application of a Ward-Tordai transient model and of a Langmuir saturation model showed that for fine-bubbles in low molecular weight surfactant solutions the interfacial surfactant accumulation equilibrates before bubble detachment.

Lioumbas *et al.* (2006) studied the effect of a non-ionic surfactant additive on the gas-liquid flow in inclined pipes. The surfactant additive strongly influenced both the interfacial characteristics and the flow field within the liquid layer. The flow patterns depended on the surfactant chemical structure rather than the surface tension alone. The appearance of the interfacial waves was delayed along with significant drag reduction.

Rozenblit *et al.* (2006) studied the flow patterns, the drag reduction, and the heat transfer in a vertical upward air-water flow with surfactant in a tube of 2.5 cm in diameter. The addition of surfactant reduced significantly the tendency of coalescence between air bubbles. The bubbles were smaller in size but higher in number than in pure air-water mixture at all flow regimes.

Wilkens *et al.* (2006) studied the effect of surfactant in a horizontal air-water pipe flow. Addition of the surfactant to the gas liquid flow significantly reduced the occurrence of the slug flow. The slug flow regime was largely replaced by a new stratified flow pattern at high liquid flow rates. These stratified flows had a layer of bubbles that appear to dampen wave growth and stabilize the interface. Surface tension was not the lone driving factor for the slug flow suppression but it appeared to be related to the tendency to foam. No surface tension effect was observed for the annular or dispersed bubble transitions.

In our work, we are interested in investigating the effects of cationic surfactant concentration and the cationic surfactant carbon tail length on the flow regimes, the corresponding pressure gradients, the bubble/slug sizes, and the bubble/slug velocities of a vertical two-phase flow

5.3 Experimental Apparatus

The experimental setup is shown schematically in Figure 1. Air, water, octylbenzyldimethylammonium chloride (C_8H_{17}-$C_9H_{13}NCl$) solutions (LEVENOL DM-08A, 46.6 wt.%, Kao), with the critical micelle concentration (CMC) equal to 61.5 g/L, at 1, 2 and 3 CMC, and hexadecylbenzyldimethylammonium chloride ($C_{16}H_{33}$-$C_9H_{13}NCl$) solution (LEVENOL RC, 49.6 wt.%, Kao), with the critical micelle concentration (CMC) equal to 0.36 g/L, at 1 CMC were used as the working fluids. The main components of the system consist of the vertical test section, an air supply, liquid supply and instrumentation. The pipe, with 1.9 cm inside diameter and the length of 300 cm was used. The pipe was made from transparent acrylic glass to permit visual observation of the flow patterns. At the bottom of the test column, there was an inlet for the compressed air from a compressor (Fu Sheng, HTA-100H, Taiwan) and flow rates were measured by a calibrated air-rotameters (1. Cole-

Parmer, A-32466-66, U.S.A., 2. Cole-Parmer, A-32466-68, U.S.A., 3. Cole-Parmer, A-32466-70, U.S.A.). Liquid was pumped from the storage tank through a rotameter and mixed with air at the bottom of the test column. The flow rate of the liquid was measured by a calibrated liquid-rotameter (Cole-Parmer, U.S.A, A-32461-42). Liquid flowed upward through the main column with air and then flowed back to the storage tank. Two static pressure tabs in each column were installed at two axial locations with spacing of 0.4 m and were connected to a manometer which was used to measure the pressure drops along the test section. The physical properties of the liquid used in the experiment are listed in Table 1.

Experiments were conducted by varying the air and liquid flow rates. The air flow rate was increased by small increments while the liquid flow rate was kept constant. The experimental conditions were as follows: air Reynolds number Re_{air}: 3.14-71,275, liquid Reynolds number Re_{liquid}: 0-2,740. Definitions of Re_{air} and Re_{water} are as defined in Table 1. Air and liquid temperatures were between ~31-32°C. The system was allowed to approach a steady state condition before any data were taken. The pressure drops across the test section were measured at different flow rates of air and liquid; average values were computed and reported from at least 5 readings. The flow regimes were observed and identified by visual observation: a video camera (Panasonic, NV-M3000) and a software program (Snagit 8.0). Bubble size, slug size and void fraction of the Taylor bubble were identified and measured by a software program (Scion Image). Bubble velocity was measured by timing bubbles traveling past known distances. Bubble and Taylor sizes and velocity were measured from 3-5 samples, and average values were computed and reported.

5.4 Results and Discussion

Physical Properties of the Liquids

Table 1 lists the values of the dynamic viscosity, the kinematic viscosity, the density, the electrical conductivity, and the surface tension of water, the octylbenzyldimethylammonium chloride solutions (C_8H_{17}-$C_9H_{13}NCl$) at concentrations of 1 CMC, 2 CMC and 3 CMC, and the hexadecylbenzyldimethyl-

ammonium chloride solution ($C_{16}H_{33}$-$C_9H_{13}NCl$) at concentration of 1 CMC. CMC here refers to the critical micelle concentration where the micelle structure starts to form at and beyond this concentration. CMC was determined from the measurements of electrical conductivity and surface tension vs. concentration. Abrupt changes in electrical conductivity and surface tension vs. concentration are identified as the CMC for the (C_8H_{17}-$C_9H_{13}NCl$) solution to be equal to 61.5 g/L (~61500 ppm), and for the ($C_{16}H_{33}$-$C_9H_{13}NCl$) solution to be equal to 0.36 g/L (~360 ppm). The viscosity of the (C_8H_{17}-$C_9H_{13}NCl$) solution changes from 8.48×10^{-4} Pa.s to 1.317×10^{-3} Pa.s, about 55 %, as concentration varies from 0 to 3 CMC. The dynamic viscosity of the (C_8H_{17}-$C_9H_{13}NCl$) solution at 1 CMC changes from 9.73×10^{-4} Pa.s to 1.103×10^{-3} Pa.s, about 13 %, as the tail length changes from that of (C_8H_{17}-$C_9H_{13}NCl$) to ($C_{16}H_{33}$-$C_9H_{13}NCl$) at 1CMC. The density of the (C_8H_{33}-$C_9H_{13}NCl$) solution changes slightly from 995 kg/m3 to 998.3 kg/m^3, about 0.33 % as concentration varies from 0 to 3 CMC. The density of the (C_8H_{17}-$C_9H_{13}NCl$) solution at 1 CMC changes from 998 kg/m^3 to 997.3 kg/m^3, about 0.07 %, as the tail length changes from that of (C_8H_{17}-$C_9H_{13}NCl$) to ($C_{16}H_{33}$-$C_9H_{13}NCl$) at 1CMC. The two surfactants change the surface tension of pure water from 71.27 mN/m to ~32 mN/m, a reduction about 55 % as concentration varies for 0 to 3 CMC.

Visual Observations of the Flow Regimes by Photographs

The air flow rate was increased while the liquid flow rate was kept fixed. The boundaries between flow regimes were designated to be the transitions towards the bubble-slug, the slug, the slug-churn, the churn, the annular, and the mist flow regimes, respectively. Each flow regime boundary was identified by observations through the video camera. Table 2 shows the critical Reynolds numbers, $Re_{air,critical}$, for each flow regime of the (C_8H_{17}-$C_9H_{13}NCl$) solution at 1 CMC at various liquid flow rates or Re_{liquid}. $Re_{air,critical}$ values for the bubble-slug and the slug flow regimes are: 8.12 and 20.49 at $Re_{liquid} = 0$; 13.07 and 28.08 at $Re_{liquid} = 1001$; and 33.21 and 43.46 at $Re_{liquid} = 2749$. It is evident that $Re_{air,critical}$ for the bubble-slug and slug flow regimes increases with increasing liquid flow rate or Re_{liquid}.

Table 3 shows the critical Reynolds numbers, $Re_{air,critical}$, for each flow regime of pure water and the (C_8H_{17}-$C_9H_{13}NCl$) solutions at various concentrations and at fixed $Re_{liquid} \sim 2{,}700$. $Re_{air,critical}$ values for the bubble-slug and the slug flow regimes are: 38.33 and 48.59 for pure water, 33.21 and 43.46 for the (C_8H_{17}-$C_9H_{13}NCl$) solution at 1 CMC; 38.33 and 43.46 for the (C_8H_{17}-$C_9H_{13}NCl$) solution at 2 CMC; and 38.33 and 43.46 for the (C_8H_{17}-$C_9H_{13}NCl$) solution at 3 CMC. $Re_{air,critical}$ value for the bubble-slug flow regime of the (C_8H_{17}-$C_9H_{13}NCl$) solution at 1 CMC is slightly lower than those of pure water and the (C_8H_{17}-$C_9H_{13}NCl$) solutions at 2 CMC and 3 CMC. $Re_{air,critical}$ value for the slug flow regime of pure water is clearly higher than those of the (C_8H_{17}-$C_9H_{13}NCl$) solutions at 1, 2, and 3 CMC, presumably due to the difference in Eo number. For other flow regimes, from the slug-churn to the mist flow regimes, the $Re_{air,critical}$ values for pure water and the (C_8H_{17}-$C_9H_{13}NCl$) solutions at various concentrations are the same. Surfactant addition and its concentration have no effect on $Re_{air,ciritical}$ in these regimes.

Table 4 shows the critical Reynolds numbers, $Re_{air,critical}$, of various flow regimes for the (C_8H_{17}-$C_9H_{13}NCl$) solution and the ($C_{16}H_{33}$-$C_9H_{13}NCl$) solution which differ in their carbon tail lengths. At $Re_{liquid} \sim 2{,}700$, $Re_{air,critical}$ for the bubble-slug and the slug flow regimes are 33.21 and 43.46 for the (C_8H_{17}-$C_9H_{13}NCl$) solution at 1 CMC, and 38.33 and 48.59 for the ($C_{16}H_{33}$-$C_9H_{13}NCl$) solution at 1 CMC. Evidently, $Re_{air,critical}$ for bubble-slug and slug flow regimes depend on the carbon tail length. For other flow regimes, from the slug-churn to the mist flow regimes, $Re_{air,critical}$ values for both (C_8H_{17}-$C_9H_{13}NCl$) and ($C_{16}H_{33}$-$C_9H_{13}NCl$) solutions are nearly the same.

Effect of Surfactant on the Pressure Gradient

Figure 2(a) shows the dynamic pressure gradients, $(-dp/dz)_d$, for the (C_8H_{17}-$C_9H_{13}NCl$) solution at 1 CMC vs. air Reynolds number, Re_{air}, at Re_{liquid} equal to 0, 1,000 and 2,700. The dynamic pressure gradient can be written as:

$$(-\frac{dp}{dz})_d = (\frac{\Delta P}{L})_d = (\frac{\Delta P}{L})_m + \rho_l g\,, \qquad (1)$$

where $(\frac{\Delta P}{L})_m$ is the measured pressure gradient along a vertical distance L between the pressure taps, ρ_l is the liquid density, and g is the gravity. The dynamic pressure gradients increase steadily with increasing Re_{air} from the bubble flow regime to the slug flow regime. In the churn flow regime, the dynamic pressure gradients are nearly constant, independent of Re_{air}. In the annular flow regime and the mist flow regime, the dynamic pressure gradients decrease with increasing air Reynolds numbers. The dynamic pressure gradient for $Re_{liquid} = 0$ is higher than those of $Re_{liquid} = 1{,}000$ and $Re_{liquid} = 2{,}700$. Therefore, the dynamic pressure gradient of the (C_8H_{17}-$C_9H_{13}NCl$) solution at 1 CMC decreases with increasing liquid flow rate.

Figure 2(b) shows the dynamic pressure gradients, $(-dp/dz)_d$, vs. air Reynolds number, Re_{air}, of the (C_8H_{17}-$C_9H_{13}NCl$) solution at various concentrations and at the same liquid Reynolds number of ~2,700. In the bubble flow regime, the dynamic pressure gradients of pure water is clearly lower than those of the (C_8H_{17}-$C_9H_{13}NCl$), solutions, presumably due to the difference in Eotvos numbers in which they differ by a factor of two. In the slug to the churn flow regimes, the dynamic pressure gradients of pure water and the (C_8H_{17}-$C_9H_{13}NCl$) solutions at various concentrations are nearly the same. In the annular flow regime and the mist flow regime, the dynamic pressure gradient of pure water is higher than those of the (C_8H_{17}-$C_9H_{13}NCl$) solutions. The (C_8H_{17}-$C_9H_{13}NCl$) solutions contain foams in these flow regimes. In addition, the flows are highly turbulent; turbulent drag reduction may occur. The dynamic pressure gradients of the (C_8H_{17}-$C_9H_{13}NCl$) solutions at various concentrations (1 CMC, 2 CMC and 3 CMC) are nearly the same spanning from the bubble flow regime to the mist flow regime.

Figure 2(c) shows the dynamic pressure gradients, $(-dp/dz)_d$, vs. air Reynolds number, Re_{air}, of the (C_8H_{17}-$C_9H_{13}NCl$) and ($C_{16}H_{33}$-$C_9H_{13}NCl$) solutions at 1 CMC and pure water at the same liquid Reynolds number of ~2,700. In the bubble flow regime, the dynamic pressure gradient of the (C_8H_{17}-$C_9H_{13}NCl$) solution is lower than that of the ($C_{16}H_{33}$-$C_9H_{13}NCl$) solution. This suggests the direct influence of the carbon tail length on the pressure gradient since the Eotvos number and the Y parameter of both solutions are nearly the same. A longer carbon tail length increases the van der Waal interaction between the surfactant molecules and

the tube wall, in addition to the slight difference in the dynamic viscosity (Table 1). It is possible that ($C_{16}H_{33}$-$C_9H_{13}NCl$) molecules absorb on the tube wall more easily than (C_8H_{17}-$C_9H_{13}NCl$) surfactants and they induce an additional wall shear stress. Therefore, in the bubble flow regime, the dynamic pressure gradient increases with increasing surfactant carbon tail length. In the slug flow regime and the churn flow regimes, the dynamic pressure gradients of water, the (C_8H_{17}-$C_9H_{13}NCl$) solution, and the ($C_{16}H_{33}$-$C_9H_{13}NCl$) solution are nearly the same. In the annular and the mist flow regimes, the pressure gradients of the (C_8H_{17}-$C_9H_{13}NCl$) and ($C_{16}H_{33}$-$C_9H_{13}NCl$) solutions are nearly the same; but they are lower than that of pure water, presumably due to the effect of turbulent drag reduction.

Figure 3(a) shows the dimensionless pressure gradients, $2d(-dp/dz)_d/\rho_w u_l^2$, of the ($C_8H_{17}$-$C_9H_{13}NCl$) solution at 1 CMC vs. air Reynolds number, Re_{air}, at various Re_{liquid} equal to ~ 1,000 and 2,700. We may define the dynamic wall shear stress ($\tau_{w,d}$):

$$\frac{d}{4}\left(\frac{\Delta P}{L}\right)_d = \tau_{w,d}, \tag{2}$$

where $\left(\frac{\Delta P}{L}\right)_d$ is the dynamic pressure drop along a distance L between the pressure taps. From the definition of the Darcy friction factor (f_F) (Wilkes (1999)):

$$f_F = \frac{8\tau_{w,d}}{\rho_w \bar{u}_{liq}^2}, \tag{3}$$

where $\bar{u}_{liq}$ is liquid velocity defined as:

$$\bar{u}_{liq} = \frac{4Q_L}{\pi d^2}, \tag{4}$$

where Q_L is the liquid volume flow rate. The friction factor for a two phase flow can be written in terms of the dimensionless pressure gradient as:

$$f_F = \frac{2d\left(-\frac{dp}{dz}\right)_d}{\rho_w \bar{u}_{liq}^2}, \tag{5}$$

From the bubble flow regime to the slug flow regime, the dimensionless pressure gradients at Re_{liquid} ~ 1,000 and 2,700 increases with increasing Re_{air}. In the churn flow regime the dimensionless pressure gradients are nearly constant, independent of Re_{air}. But in the annular and the mist flow regimes, the dimensionless pressure gradients decrease with increasing air flow rate or Re_{air}. Furthermore, the dimensionless pressure gradient for Re_{liquid} = 1,000 is higher than that of Re_{liquid} = 2,700. This evidently suggests the influence of Re_{liquid}.

Figure 3(b) shows the dimensionless pressure gradients, $2d(-dp/dz)_d/\rho_w u_l^2$, vs. air Reynolds number, Re_{air}, of the (C_8H_{17}-$C_9H_{13}NCl$) solutions at various concentrations and of pure water at the same liquid Reynolds number of ~2,700. In the bubble flow regime, the dimensionless pressure gradient of pure water is lower than those of the (C_8H_{17}-$C_9H_{13}NCl$) solutions of 1, 2 and 3 CMC. This is likely a result caused the differences in bubble sizes, the Eotvos number, Eo, and marginally the property parameter, Y. For pure water, Eo and Y are equal to 49.44 and 1.41 x 10^{-11}; these are lower than Eo and Y of the (C_8H_{17}-$C_9H_{13}NCl$) solution at 1 CMC which are ~ 115 and ~ 3.1 x 10^{-10}, respectively. In the slug to the mist flow regimes, the dimensionless pressure gradients of the (C_8H_{17}-$C_9H_{13}NCl$) solutions of various concentrations are lower than that of pure water. Adding surfactant evidently produces a lower dimensionless pressure gradient; this is probably due to the effect of turbulent drag reduction.

Figure 3(c) shows the dimensionless pressure gradients, $2d(-dp/dz)_d/\rho_w u_l^2$, vs. air Reynolds number, Re_{air}, of the (C_8H_{17}-$C_9H_{13}NCl$) and ($C_{16}H_{33}$-$C_9H_{13}NCl$) solutions at 1 CMC and of pure water at the same liquid Reynolds number of ~2,700. In the bubble flow regime, the dimensionless pressure gradient of the (C_8H_{17}-$C_9H_{13}NCl$) solution is lower than those of the ($C_{16}H_{33}$-$C_9H_{13}NCl$) solution, possibly due to the difference in the dynamic viscosity since Eotvos numbers are essentially the same. In the bubble flow regime, the dimensionless pressure gradient of pure water is lower than those of both surfactant solutions due to the differences in the dynamic viscosity and Eotvos number. In the slug, the churn, the annular, and the mist flow regime, the dimensionless pressure gradients of both surfactant solutions are clearly lower than that of pure water; this may arise from the differences in

Eotvos number, the foaming of both surfactant solutions, and possibly the turbulent drag reduction effect.

Effect of Surfactants on the Bubble and the Slug Sizes

Figures 4(a) to 4(e) show photographs of bubble flows of the surfactant solutions of various concentrations and of pure water, all at Re_{air} = 28.08 and Re_{liquid} ~ 2,700. Figure 4(a) shows a photograph of the bubble flow of the (C_8H_{17}-$C_9H_{13}NCl$) solution at 1 CMC, Eo = 115, Y = 3.06 x 10^{-10}. Figure 4(b) shows a photograph of the bubble flow of the (C_8H_{17}-$C_9H_{13}NCl$) solution at 2 CMC, Eo = 104, Y = 5.06 x 10^{-10}. Figure 4(c) shows a photograph of the bubble flow in the (C_8H_{17}-$C_9H_{13}NCl$) solution at 3 CMC, Eo = 98.62, Y = 6.42 x 10^{-10}. Figure 4(d) shows a photograph of the bubble flow of the ($C_{16}H_{33}$-$C_9H_{13}NCl$) solution at 1 CMC, Eo = 113, Y = 4.74 x 10^{-10}. Figure 4(e) shows a photograph of the bubble flow in pure water, Eo = 49.44, Y = 1.41 x 10^{-11}. The shape of the bubble of pure water appears as a spherical cap on top of a cylinder and it covers all of cross section area. For the (C_8H_{17}-$C_9H_{13}NCl$) solutions at 1, 2, 3 CMC and the ($C_{16}H_{33}$-$C_9H_{13}NCl$) solution at 1 CMC, the shapes of air bubbles appear as a spherical cap with cylinder but they do not fill all of cross section area.

Figures 5(a) shows the normalized bubble widths, w_b/d, for the (C_8H_{17}-$C_9H_{13}NCl$) solution at 1 CMC vs. air Reynolds number, Re_{air}, at Re_{liquid} = 0, ~1,000 and ~2,700. The bubble width increases slightly with increasing Re_{air} or increasing air flow rate. The bubble width for Re_{liquid} = 2,700 is lower than those of Re_{liquid} = 0 and 1,000.

Figure 5(b) shows the bubble width, w_b/d, of pure water and the (C_8H_{17}-$C_9H_{13}NCl$) solutions at various concentrations vs. air Reynolds number, Re_{air}, at the same liquid Reynolds number of ~2,700. The bubble width for pure water is higher than those of the (C_8H_{17}-$C_9H_{13}NCl$) solutions at 1 CMC, 2 CMC and 3 CMC. The surfactants reduces the surface tension and thus promote the breakup of air bubbles, therefore, the bubbles of the surfactant solutions are smaller in size. Furthermore, the normalized bubble widths of the (C_8H_{17}-$C_9H_{13}NCl$) solutions at three concentrations

are nearly the same, despite the differences in the Eotvos number and the Y parameter.

Figure 5(c) shows the bubble width, w_b/d, vs. air Reynolds number, Re_{air}, of the (C_8H_{17}-$C_9H_{13}NCl$) solution at 1 CMC, the ($C_{16}H_{33}$-$C_9H_{13}NCl$) solution at 1 CMC, and pure water at the same liquid Reynolds number of ~2,700. The normalized bubble width of the (C_8H_{17}-$C_9H_{13}NCl$) solution is nearly the same as that of the ($C_{16}H_{33}$-$C_9H_{13}NCl$) solution, implying the carbon tail length has no apparent effect on the bubble width, and the corresponding Eotvos numbers are nearly the same. On the other hand, the bubble width for pure water is larger than those of the (C_8H_{17}-$C_9H_{13}NCl$) solution and the ($C_{16}H_{33}$-$C_9H_{13}NCl$) solution.

Figure 6(a) shows the normalized bubble height, R_h/d, of the (C_8H_{17}-$C_9H_{13}NCl$) solution at 1 CMC vs. air Reynolds number, Re_{air}, at Re_{liquid} = 0, ~1,000 and ~2,700. The bubble height generally increases with increasing Re_{air}, consistent with the conservation of air flow rate. The normalized bubble height for Re_{liquid} = 0 is lower than that of Re_{liquid} = 1,000, suggesting that the bubble height is expanded further by the co-flowing liquid velocity. The normalized bubble height for Re_{liquid} = 2,700 is, however, even lower than that of Re_{liquid} = 0 and 1,000; a high liquid flow rate may possibly reduce the tendency to coalescence between air bubbles. In summary, at Re_{liquid} = 1,000, the bubble height is expanded as the liquid velocity plays more a pronounced role than the reduction of coalescence between air bubbles at the high liquid flow.

Figure 6(b) shows the normalized bubble heights, R_h/d, of pure water and the (C_8H_{17}-$C_9H_{13}NCl$) solutions at various concentrations vs. air Reynolds number, Re_{air}, at the same liquid Reynolds number of ~2,700. The bubble height for pure water is higher than those of the (C_8H_{17}-$C_9H_{13}NCl$) solutions at 1 CMC, 2 CMC and 3 CMC because the surfactant reduces the surface tension and the tendency to coalescence between air bubbles. The normalize bubble heights of the (C_8H_{17}-$C_9H_{13}NCl$) solutions at three concentrations are nearly the same implying surfactant concentration has no apparent effect on the bubble height.

Figure 6(c) shows the normalized bubble height, R_h/d, vs. air Reynolds number, Re_{air}, of the (C_8H_{17}-$C_9H_{13}NCl$) solution at 1 CMC, the ($C_{16}H_{33}$-$C_9H_{13}NCl$) solution at 1 CMC, and pure water at the same liquid Reynolds number of ~2,700.

The normalized bubble height for the (C_8H_{17}-$C_9H_{13}NCl$) solution is nearly the same with that of the ($C_{16}H_{33}$-$C_9H_{13}NCl$) solution, implying the carbon tail length has no apparent effect on the bubble height.

Figure 7(a) shows the normalized slug height, L_{TB}/d, of the (C_8H_{17}-$C_9H_{13}NCl$) solution at 1 CMC vs. air Reynolds number, Re_{air}, of various Re_{liquid} = 0, ~1,000 and ~2,700. The normalized slug height for Re_{liquid} = 0 is greater than that of Re_{liquid} = 1,000 which in turn is greater than that Re_{liquid} = 2,700; this may arise because an increase in the liquid flow rate may inhibit coalescence between air slugs.

Figure 7(b) shows the normalized slug height, L_{TB}/d, of pure water and the (C_8H_{17}-$C_9H_{13}NCl$) solution at various concentrations vs. air Reynolds number, Re_{air}, at the same liquid Reynolds number of ~2,700. At low Re_{air}, the normalized slug height of pure water is nearly the same as those of (C_8H_{17}-$C_9H_{13}NCl$) solutions at 1 CMC, 2 CMC and 3 CMC. But at high Re_{air}, the normalized slug height of pure water is higher than those of the (C_8H_{17}-$C_9H_{13}NCl$) solutions. The normalized slug height of the (C_8H_{17}-$C_9H_{13}NCl$) solution at 1 CMC is lower than that of the (C_8H_{17}-$C_9H_{13}NCl$) solution at 2 CMC, and the normalized slug height of the (C_8H_{17}-$C_9H_{13}NCl$) solution at 2 CMC is lower than that of the (C_8H_{17}-$C_9H_{13}NCl$) solution at 3 CMC. The slug height increases with increasing (C_8H_{17}-$C_9H_{13}NCl$) concentration, implying the effect of reduced surface tension or the difference in Eotvos number.

Figure 7(c) shows the normalized slug height, L_{TB}/d, vs. air Reynolds number, Re_{air}, of the (C_8H_{17}-$C_9H_{13}NCl$) solution at 1 CMC, the ($C_{16}H_{33}$-$C_9H_{13}NCl$) solution at 1 CMC, and pure water at the same liquid Reynolds number of ~2,700. At low Re_{air}, the normalized slug height of the (C_8H_{17}-$C_9H_{13}NCl$) solution is nearly the same as that of the ($C_{16}H_{33}$-$C_9H_{13}NCl$) solution. But at high Re_{air}, the normalized slug height of the (C_8H_{17}-$C_9H_{13}NCl$) solution is lower than that of the ($C_{16}H_{33}$-$C_9H_{13}NCl$) solution. The slug height increases with increasing carbon tail length, only at high air flow rates.

Effect of Surfactants on the Bubble and the Slug Velocities

Figures 8(a) shows the normalized bubble and slug velocity, $\frac{u}{\sqrt{gd}}$, of the (C_8H_{17}-$C_9H_{13}NCl$) solution at 1 CMC vs. air Reynolds number, Re_{air}, at Re_{liquid} = 0, ~1,000 and ~2,700. The normalized bubble and slug velocities at each Re_{liquid} increase with increasing Re_{air}, consistent with the conservation of air flow rate. The bubble and slug velocities for Re_{liquid} = 2,700 are higher than those at Re_{liquid} = 1,000 which in turn are higher than those at Re_{liquid} = 0, evidently due to effect on increasing the liquid flow rate.

Figure 8(b) shows the normalized bubble and slug velocities, $\frac{u}{\sqrt{gd}}$, of pure water and the (C_8H_{17}-$C_9H_{13}NCl$) solutions at various concentrations vs. air Reynolds number, Re_{air}, at the same liquid Reynolds number of ~2,700. The bubble and slug velocities at 1 CMC, 2 CMC and 3 CMC are higher than that of pure water due to the surface tension effect or the difference in Eotvos number. The bubble and slug velocities of the solution at 3 CMC are slightly higher than those of the solution at 2 CMC which are in turn slightly higher than those of the solution at 1 CMC. Therefore, the bubble and slug velocities increase with increasing surfactant concentration.

Figure 8(c) shows the normalized bubble and slug velocity, $\frac{u}{\sqrt{gd}}$, vs. air Reynolds number, Re_{air}, of the (C_8H_{17}-$C_9H_{13}NCl$) solution at 1 CMC, the ($C_{16}H_{33}$-$C_9H_{13}NCl$) solution at 1 CMC, and pure water at the same liquid Reynolds number of ~2,700. The normalized bubble and slug velocity of the (C16H33-C9H13NCl) solution is slightly higher than those of the (C_8H_{17}-$C_9H_{13}NCl$) solution because an increase in the carbon tail length increases the van der Waal interaction between the surfactant on the tube wall. The long carbon tail length surfactant can absorb more easily onto the tube surface more than the short carbon tail length surfactant, inducing the bubble and slug velocities to increase with increasing carbon tail length.

5.5 Conclusions

The experiments were carried out on the two-phase upward flows consisting a gas and a liquid in a vertical tube with an inner diameter 0.019 m and a length of 3 m. The working fluids were air-water, air-(C_8H_{17}-$C_9H_{13}NCl$) solution, and air-($C_{16}H_{33}$-$C_9H_{13}NCl$) solution in order to investigate the influence of surfactant addition on the flow regimes, the corresponding pressure gradients, the bubble/slug size and the velocity.

The boundaries of the bubble-slug and the slug flow regimes of the (C_8H_{17}-$C_9H_{13}NCl$) solution (1CMC) shift to the smaller values relative to those of pure water. But the boundaries for the churn, the annular and the mist flow regimes remain nearly the same. $Re_{air,critical}$ for the bubble-slug flow regime of the (C_8H_{17}-$C_9H_{13}NCl$) solution at 1 CMC is slightly lower than those of the (C_8H_{17}-$C_9H_{13}NCl$) solutions at 2 CMC and 3 CMC because of the viscosity effect. $Re_{air,critical}$ for the bubble-slug and the slug flow regimes increases slightly with increasing carbon length.

In the bubble to the slug flow regimes, the dynamic pressure gradient of pure water is lower than that of the (C_8H_{17}-$C_9H_{13}NCl$) solutions due to the effect of viscosity. From the annular flow to the mist flow regimes, the dynamic pressure gradients of pure water is higher than those (C_8H_{17}-$C_9H_{13}NCl$) solution because the (C_8H_{17}-$C_9H_{13}NCl$) solutions contain foams, the flow are highly turbulent, and the difference in Eo number. The dynamic pressure gradient increases with increasing carbon tail length in the bubble flow regime; an increase in the carbon tail length increases the van der Waal interaction between the surfactant and the tube wall, and the slight decrease in the dynamic viscosity occurs, implying that the (C_8H_{17}-$C_9H_{13}NCl$) solution is more effective in reducing the wall shear stress than the ($C_{16}H_{33}$-$C_9H_{13}NCl$) solution.

The dimensionless pressure gradient of pure water is lower than those of the (C_8H_{17}-$C_9H_{13}NCl$) solutions at 1, 2, 3 CMC in bubble flow regime because of the differences in the dynamic viscosity, the bubble size, the Eotvos, and the property parameter, Y. A higher surfactant concentration produces a lower dimensionless pressure gradient due to the turbulent drag reduction effect. The dimensionless

pressure gradient of the (C_8H_{17}-$C_9H_{13}NCl$) solution is lower than that of the ($C_{16}H_{33}$-$C_9H_{13}NCl$) solution suggesting the carbon tail length effect.

The normalized bubble or slug sizes of pure water are greater than those of the (C_8H_{17}-$C_9H_{13}NCl$) solutions and the ($C_{16}H_{33}$-$C_9H_{13}NCl$) solution because adding surfactant can reduce the surface tension and the tendency to coalescence between air bubbles. Surfactant concentration and carbon tail length have no apparent effect on the bubble sizes. At high Re_{air}, the slug height increases with increasing (C_8H_{17}-$C_9H_{13}NCl$) concentration implying the effect of reduced surface tension. The slug height increases with increasing carbon tail length due to the surfactant-wall interaction.

The normalized bubble or slug velocities of the (C_8H_{17}-$C_9H_{13}NCl$) solutions at 1, 2 and 3 CMC are higher than those of pure water, suggesting the surface tension effect. The bubble and slug velocities increase with increasing surfactant concentration. The bubble or slug velocities increase slightly with increasing carbon tail length.

5.6 Acknowledgements

AS would like to acknowledge the financial supports from the Conductive and Electroactive Polymers Research Unit and KFAS both of Chulalongkorn University, the Petroleum Petrochemical and Advanced Materials Consortium, the Royal Thai Government (Budget of Fiscal Year 2550), and TRF-BRG.

5.7 References

Barbosa, J.R., Govan, A.H., Hewitt, G.F., 2001. Visualisation and modeling studies of churn flow in a vertical pipe. International Journal of Multiphase Flow, 27, 2105-2127.

Davies, R.M., Taylor, G.I., 1950. The mechanics of large bubbles rising through extended liquids and through liquids in tubes. Proceedings of Royal. Society, 200A, 375-390.

Duangprasert, T., 2006. Vertical two-phase flow regime and pressure gradient under the influence of SDS surfactant. MS thesis, Petroleum and petrochemical college, Chulalongkorn university, Bangkok.

English, N.J., Kandliker, S.G., 2006. An experimental investigation into the effect of surfactants on air-water two-phase flow in minichannels. Heat transfer engineering, 27(4), 99-108.

Hlaing, N.D., Sirivat, A., Siemanond, K., Wilkes, J.O., 2007. Vertical two-phase flow regimes and pressure gradients: Effect of viscosity. Experimental Thermal and Fluid Science, 31, 567-577.

Kawaguchi, Y., Segawa, T., Feng, Z., Li, P., 2002. Experimental study on drag-reducing channel flow with surfactant additives-spatial structure of turbulence investigated by PIV system. International Journal of Heat and Fluid Flow, 23, 700-709.

Lioumbas, J.S., Mouza, A.A., Paras, S.V., 2006. Effect of surfactant additives on co-current gas-liquid downflow. Chemical Engineering Science, 61, 4605-4616.

Lockhart, R.W., Martinelli, R.C., 1949. Proposed correlation of data for isothermal two-phase, two-component flow in Pipes. Chemical Engineering Progress, 45(1), 39-48.

Nicklin, D.J., 1962. Two-phase bubble flow. Chemical Engineering Science, 17, 693- 702.

Rosso, D., Huo, D.L., Stenstrom, M.K., 2006. Effects of interfacial surfactant contamination on bubble gas transfer. Chemical Engineering Science, 61, 5500-5514.

Rozenblit, R., Gurevich, M., Lengel, Y., Hetsroni, G., 2006. Flow patterns and heat transfer in vertical upward air-water flow with surfactant. International Journal of Multiphase Flow, 32, 889-901.

Soleimani, A., Al-Sarkhi, A., Hanratty, T.J., 2002. Effect of drag-reducing polymers on pseudo-slugs-interfacial drag and transition to slug flow. International Journal of Multiphase Flow, 28, 1911-1927.

Sylvester, N.D., 1987. A mechanistic model for two-phase vertical slug flow in pipes. Journal of Energy Resources Technology, Transactions of the ASME, 109(4), 206-213.

Usui, H., Kamada, T., Suzuki, H., 2004. Surfactant drag reduction caused by a cationic surfactant with excess addition of counter-ions. Journal of Chemical Engineering of Japan, 37(10), 1232-1237.

Viana, F., Pardo, R., Yanez, R., Trallero, J.L., Joseph, D.D., 2003. Universal correlation for the rise velocity of long gas bubbles in round pipes. J. Fluid Mech, 494, 379-398.

Walllis, G.B. 1969. One-dimensional Two-Phase Flow, McGraw Hill, New York.

Watson, M.J., Hewitt, G.F., 1999. Pressure effects on the slug to churn transition. International Journal of Multiphase Flow, 25, 1225-1241.

White, E.T., Beardmore, R.H., 1962. The velocity of rise of single cylindrical air bubbles through liquids contained in vertical tubes. Chemical Engineering Science, 17, 351-361.

Wilkens, R.J., Thomas, D.K., Glassmeyer, S.R., 2006. Surfactant use for slug flow pattern suppression and new flow pattern types in a horizontal pipe. Journal of Fluids Engineering, Transactions of the ASME, 128, 164-169.

Wilkes, J.O. 1999. Fluid Mechanics for Chemical Engineers, Prentice-Hall PTR, New Jersey.

Xin, R.C., Awwad, A., Dong, Z.F., Ebadian, M.A., Soliman, H.M., 1996. An investigation and comparative study of the pressure drop in air-water two-phase flow in vertical helicoidal pipes. International Journal of Heat and Mass Transfer, 39(4), 735-743.

Yu, B., Li, F., Kawaguchi, Y., 2004. Numerical and experimental investigation of turbulent characteristics in a drag-reducing flow with surfactant additives. International Journal of Heat and Fluid Flow, 25, 961-974.

Zhange, Y., Qi, Y., Zakin, J.L., 2005. Headgroup effect on drag reduction and rheological properties of micellar solutions of quaternary ammonium surfactants. Rheologica Acta, 45, 42-58.

Table 1 Physical properties of the gas and the liquids used in the experiment

Gas / Liquid	C (g/L)	μ (Pa.s)	ν (m^2/s)	ρ (kg/m^3)	σ (μS/cm)	γ (mN/m)	Eo	Y
Air	-	1.85×10^{-5}	1.57×10^{-5}	1.18	-	-	-	-
Water	-	8.48×10^{-4}	8.52×10^{-7}	995	1.3	71.27	49.44	1.41×10^{-11}
(C_8H_{17}-$C_9H_{13}NCl$) (1CMC)	61.5	9.73×10^{-4}	9.75×10^{-7}	998	7240	30.66	115	3.06×10^{-1}
(C_8H_{17}-$C_9H_{13}NCl$) (2CMC)	123	1.189×10^{-3}	1.191×10^{-6}	998.3	12606	33.85	104	5.06×10^{-1}
(C_8H_{17}-$C_9H_{13}NCl$) (3CMC)	184.5	1.317×10^{-3}	1.319×10^{-6}	998.3	17781	35.85	98.62	6.42×10^{-1}
($C_{16}H_{33}$-$C_9H_{13}NCl$) (1CMC)	0.36	1.103×10^{-3}	1.106×10^{-6}	997.3	45.7	31.31	113	4.74×10^{-1}

(C_8H_{17}-$C_9H_{13}NCl$): Octylbenzyldimethylammonium chloride solution

($C_{16}H_{33}$-$C_9H_{13}NCl$): Hexadecylbenzyldimethylammonium chloride solution

C: concentration, μ: viscosity, ν: kinematic viscosity, ρ: density, σ: electrical conductivity, γ: surface tension, d : pipe diameter, and v : velocity

System temperature, T = 31°C (± 1°C)

Re_{air}: air Reynolds number ($\frac{\rho_{air} d v_{air}}{\mu_{air}}$)

Re_{liquid}: liquid Reynolds number ($\frac{\rho_{liquid} d v_{liquid}}{\mu_{liquid}}$)

Eo : Eotvos number ($\frac{\rho g d^2}{\gamma}$)

Y: property parameter ($\frac{g\mu^4}{\rho\gamma^3}$)

Table 2 The critical Reynolds numbers $(Re_{air})_{critical}$ of various regimes of octylbenzyldimethylammonium chloride solution (1CMC)

Liquid	Re_{liquid}	$Re_{air,critical}$ for each flow regime					
		Bubble-slug	Slug	Slug-churn	Churn	Annular	Mist
(C_8H_{17}-$C_9H_{13}NCl$) (1CMC)	0	8.12	20.49	-	-	-	-
(C_8H_{17}-$C_9H_{13}NCl$) (1CMC)	1001	13.07	28.08	296	1454	28510	57020
(C_8H_{17}-$C_9H_{13}NCl$) (1CMC)	2749	33.21	43.46	369	2474	28510	57020

Table 3 The critical Reynolds numbers $(Re_{air})_{critical}$ of various regimes by using water and octylbenzyldimethylammonium chloride solution (1, 2 and 3 CMC)

Liquid	Re_{liquid}	Eo	Y	$Re_{air, critical}$ for each flow regime					
				Bubble-slug	Slug	Slug-churn	Churn	Annular	Mist
Water	2740	49.44	1.41×10^{-11}	38.33	48.59	369	2474	28510	57020
(C_8H_{17}-$C_9H_{13}NCl$) (1 CMC)	2749	115	3.06×10^{-10}	33.21	43.46	369	2474	28510	57020
(C_8H_{17}-$C_9H_{13}NCl$) (2 CMC)	2731	104	5.06×10^{-10}	38.33	43.46	369	2474	28510	57020
(C_8H_{17}-$C_9H_{13}NCl$) (3 CMC)	2735	98.62	6.42×10^{-10}	38.33	43.46	369	2474	28510	57020

Table 4 The critical Reynolds numbers $(Re_{air})_{critical}$ of various regimes by using octylbenzyldimethylammonium chloride solution (1 CMC) hexadecylbenzyldimethylammonium chloride solution (1 CMC)

Liquid	Re_{liquid}	Eo	Y	$Re_{air, critical}$ for each flow regime					
				Bubble-slug	Slug	Slug-churn	Churn	Annular	Mist
(C_8H_{17}-$C_9H_{13}NCl$) (1 CMC)	2749	115	3.06×10^{-10}	33.21	43.46	369	2474	28510	57020
($C_{16}H_{33}$-$C_9H_{13}NCl$) (1CMC)	2741	113	4.74×10^{-10}	38.33	48.59	369	2474	28510	57020

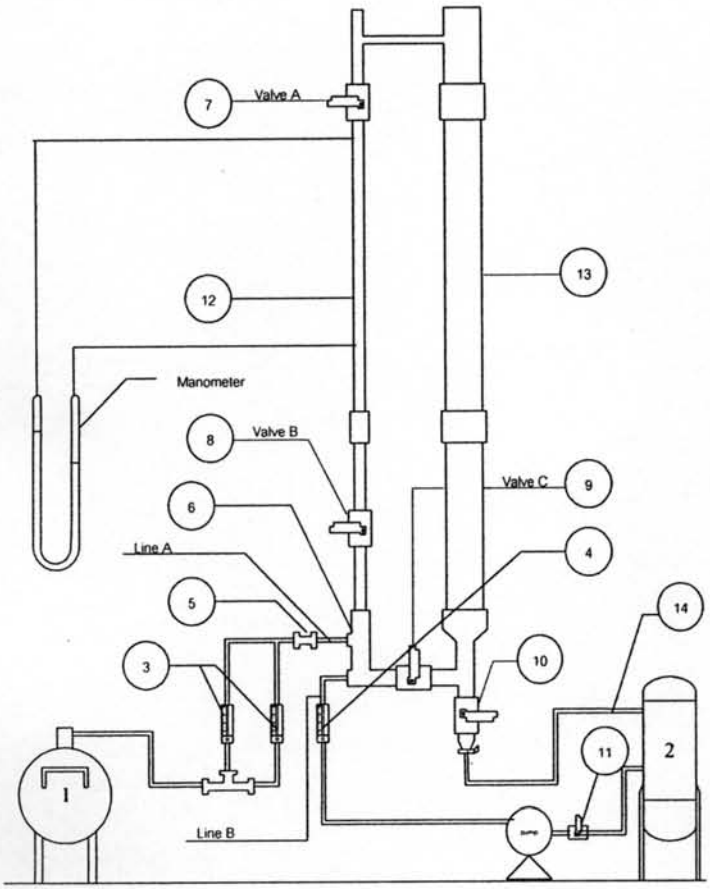

1 Air compressor maximum 10 bar
2 Solution reservoir tank
3. Air rotameter
4. liquid rotameter
5. check value
6. Air injection tee
7. Ball valve A
8. Ball valve B
9. Ball valve C
10. Draining ball valve
11. Control valve for reservoir tank
12. Acrylic tube (1.9 cm)
13. Overflow acrylic tube (5.4 cm)
14. Solution return line to reservoir
Line A Air injection line
Line B Solution injection line

Figure 1 Schematic diagram of the experimental apparatus.

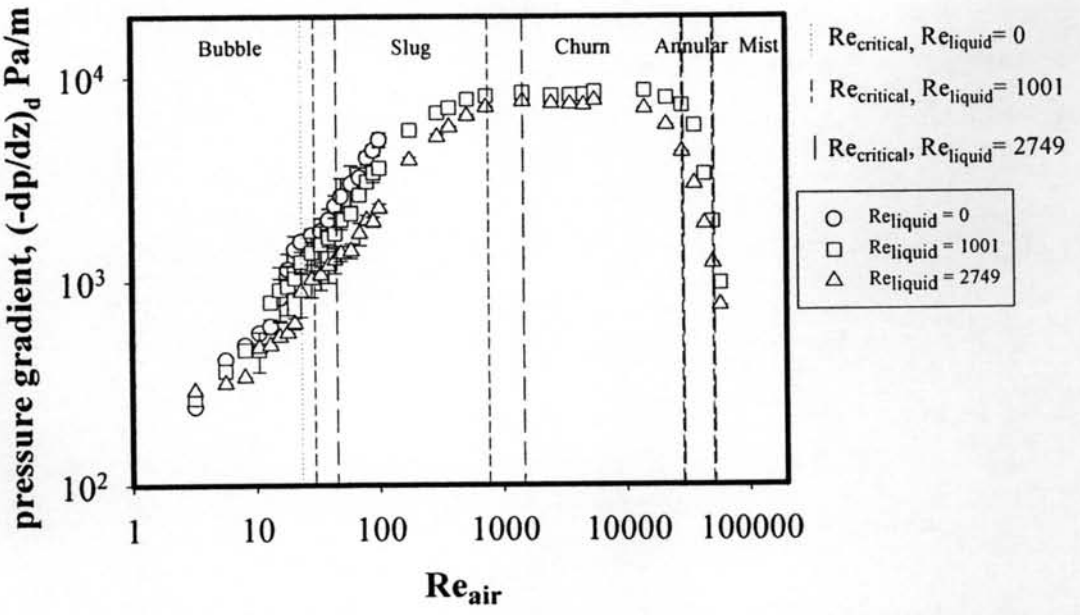

$(-dp/dz)_d$: Dynamic pressure gradient for octylbenzyldimethyl ammonium chloride surfactant (1CMC)

(a)

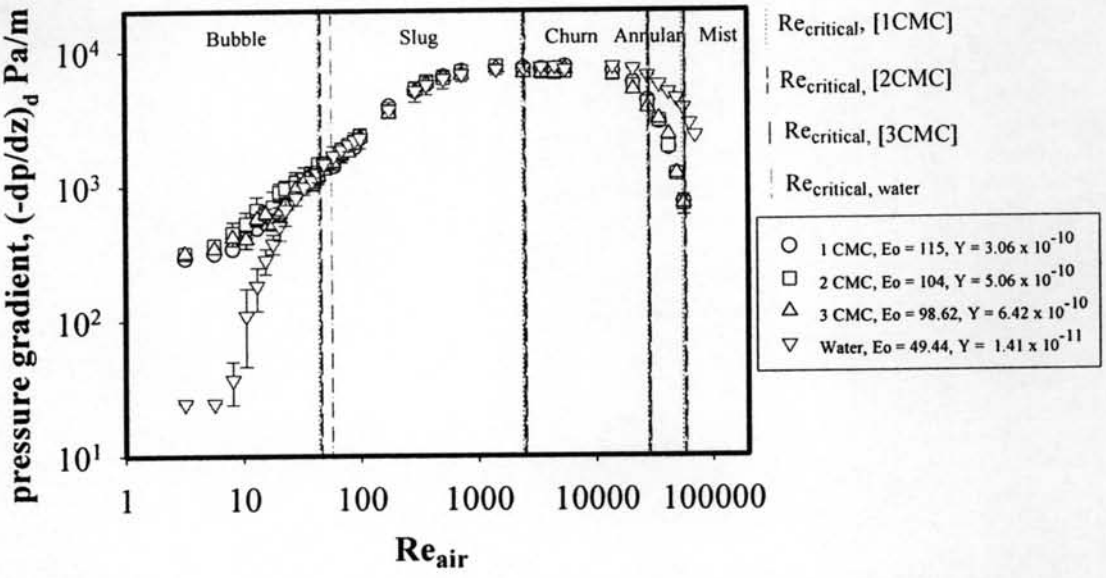

$(-dp/dz)_d$: Dynamic pressure gradient for octylbenzyldimethyl ammonium chloride surfactant and water

(b)

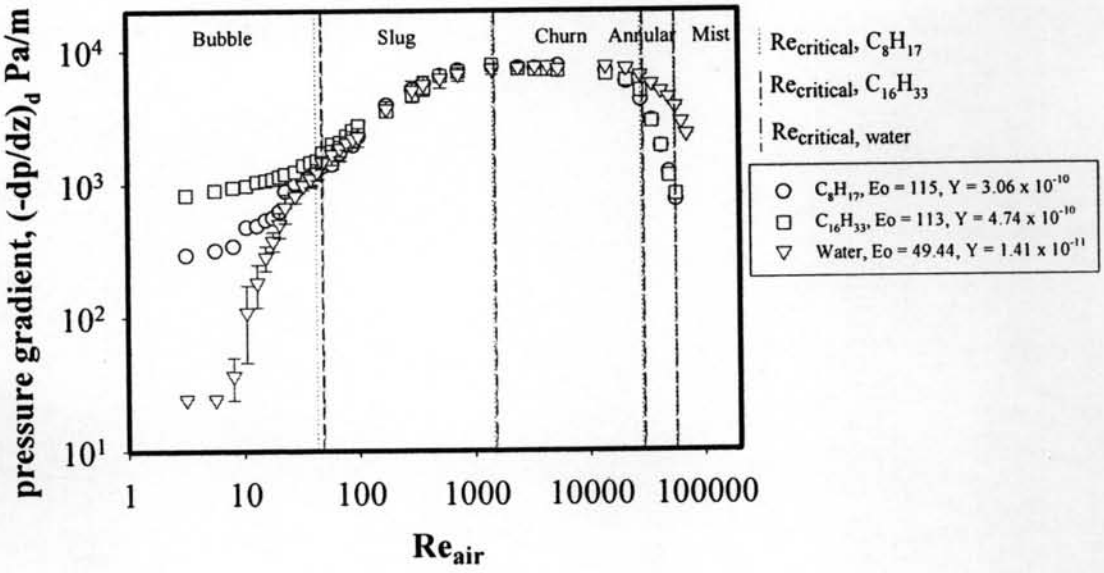

$(-dp/dz)_d$: Dynamic pressure gradient
C_8H_{17} : Octylbenzyldimethyl ammonium chloride surfactant (1CMC)
$C_{16}H_{33}$: Hexadecylbenzyldimethyl ammonium chloride surfactant (1CMC)

(c)

Figure 2 Dynamic pressure gradient vs. air Reynolds number: a) effect of Re_{liquid} = 0, 1001 and 2749, Eo = 115, Y = 3.06×10^{-10} ; b) effect of concentration, Re_{liquid} = 2749, 2731, 2735, and 2740; c) effect of carbon tail length, Re_{liquid} = 2749, 2741, and 2740.

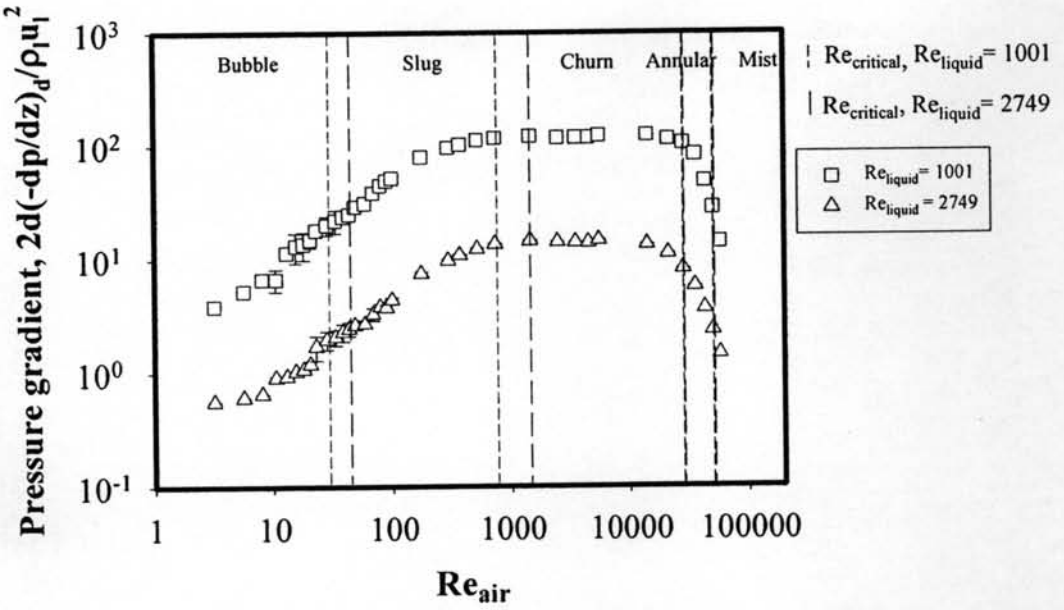

$(-dp/dz)_d$: Dynamic pressure gradient for octylbenzyldimethyl ammonium chloride surfactant (1CMC)

ρ_l : Liquid density

u_l : Mean liquid velocity, (Liquid flow rate / Cross section area)

d : Pipe diameter

(a)

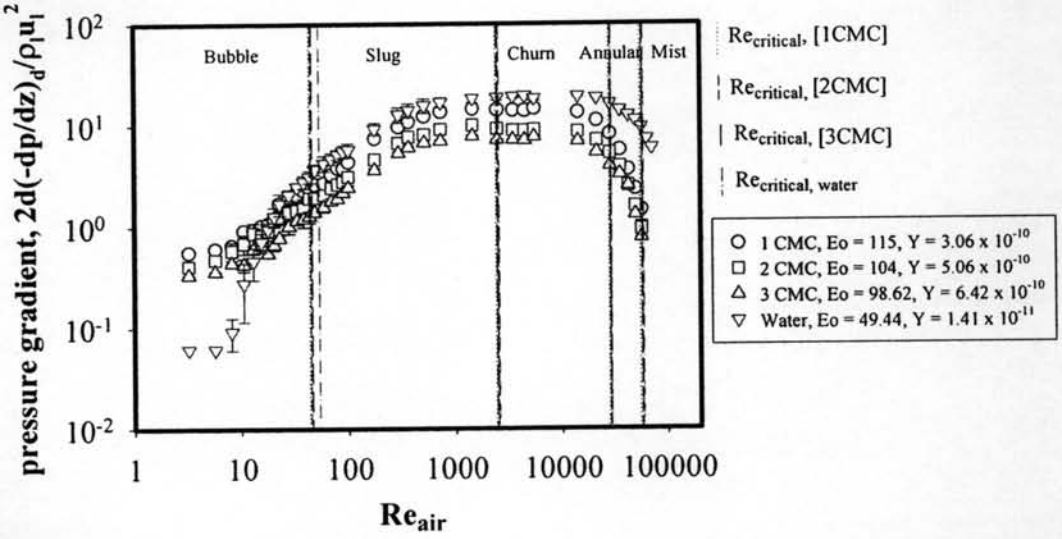

$(-dp/dz)_d$: Dynamic pressure gradient for octylbenzyldimethyl ammonium chloride surfactant and water

ρ_l : Liquid density

u_l : Mean liquid velocity, (Liquid flow rate / Cross section area)

d : Pipe diameter

(b)

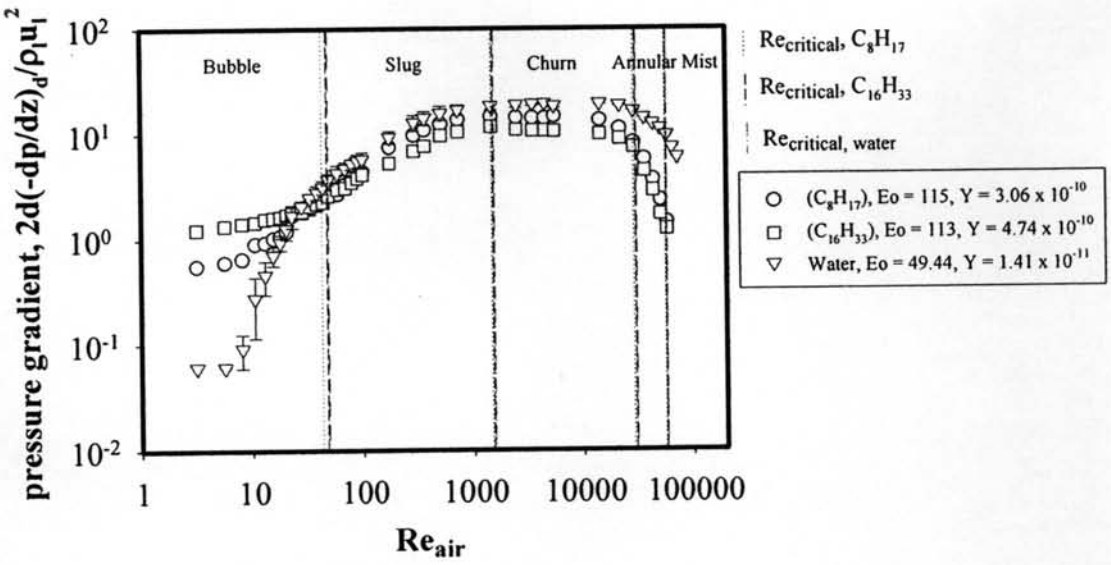

$(-dp/dz)_d$: Dynamic pressure gradient

ρ_l : Liquid density

u_l : Mean liquid velocity, (Liquid flow rate / Cross section area)

d : Pipe diameter

(C_8H_{17}) : Octylbenzyldimethyl ammonium chloride surfactant (1CMC)

$(C_{16}H_{33})$: Hexadecylbenzyldimethyl ammonium chloride surfactant (1CMC)

(c)

Figure 3 Dimensionless pressure gradient vs. air Reynolds number: a) effect of Re_{liquid}= 1001 and 2749, Eo = 115, $Y = 3.06 \times 10^{-10}$; b) effect of concentration, Re_{liquid}= 2749, 2731, 2735 and 2740; c) effect of carbon tail length, Re_{liquid}= 2749, 2741 and 2740.

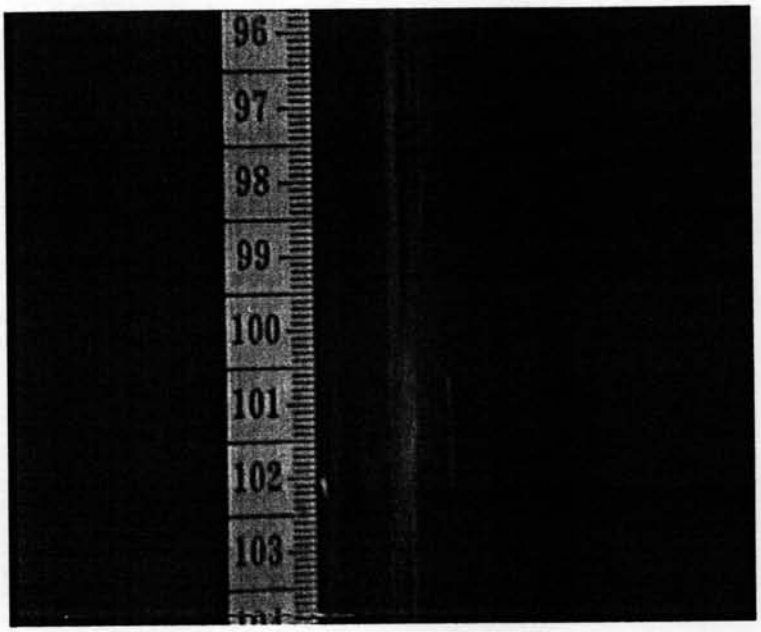

(a)

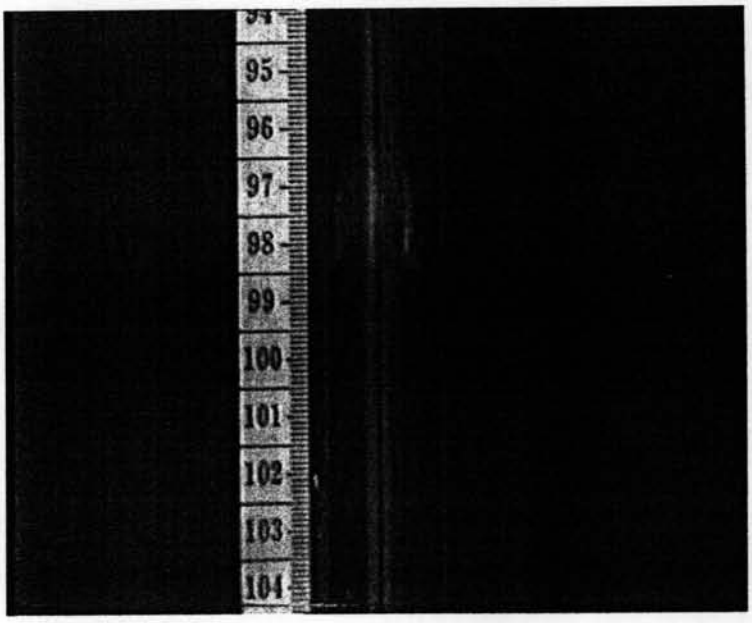

(b)

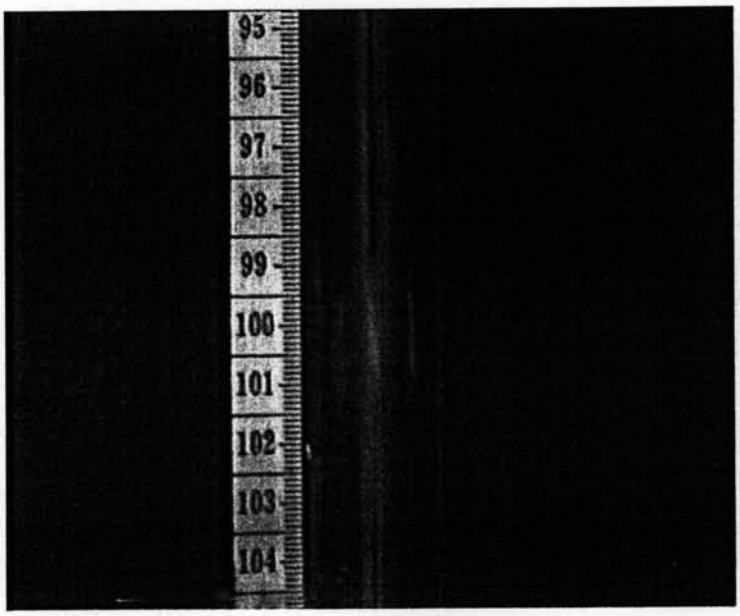
95
96
97
98
99
100
101
102
103
104

(c)

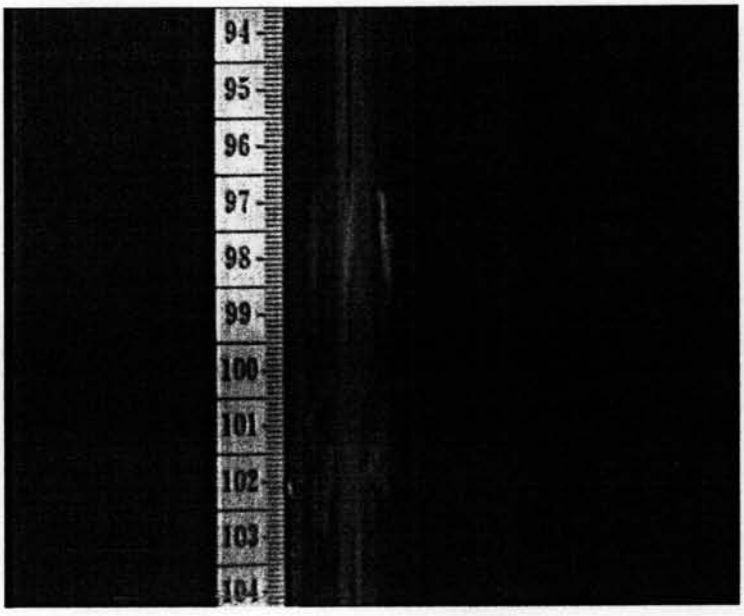
94
95
96
97
98
99
100
101
102
103
104

(d)

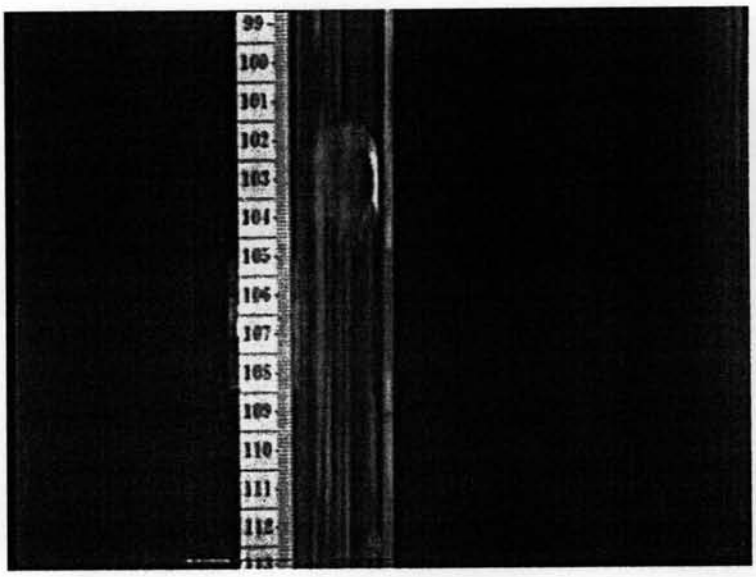

(e)

Figure 4 Photographs of bubbles in the bubble flow regime:

a) Octylbenzyldimethylammonium chloride (1CMC), Re_{air} = 28.08, Re_{liquid} = 2749, Eo = 115, Y = 3.06×10^{-10};

b) Octylbenzyldimethylammonium chloride (2CMC), Re_{air} = 28.08, Re_{liquid} = 2731, Eo = 104, Y = 5.06×10^{-10};

c) Octylbenzyldimethylammonium chloride (3CMC), Re_{air} = 28.08, Re_{liquid} = 2735, Eo = 98.62, Y = 6.42×10^{-10};

d) Hexadecylbenzyldimethylammonium chloride(1CMC), Re_{air} = 28.08, Re_{liquid} = 2741, Eo = 113, Y = 4.74×10^{-10};

e) Pure water, Re_{air} = 28.08, Re_{liquid} = 2740, Eo = 49.44, Y = 1.41×10^{-11}.

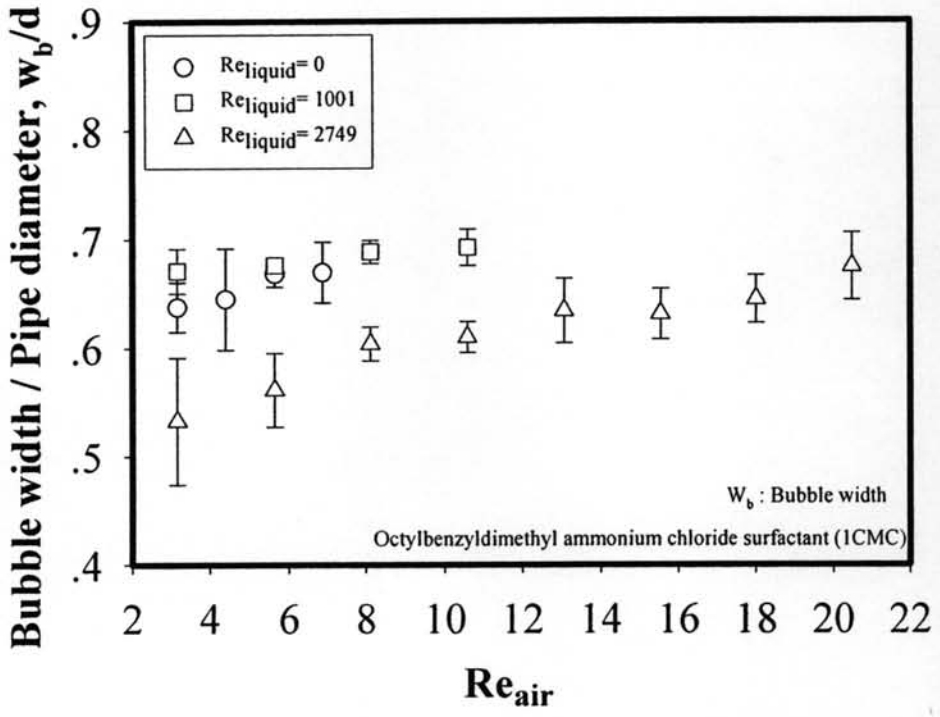
Bubble width / Pipe diameter, w_b/d
.9
.8
.7
.6
.5
.4
Re_{liquid}= 0
Re_{liquid}= 1001
Re_{liquid}= 2749
W_b : Bubble width
Octylbenzyldimethyl ammonium chloride surfactant (1CMC)
2 4 6 8 10 12 14 16 18 20 22
Re_{air}

(a)

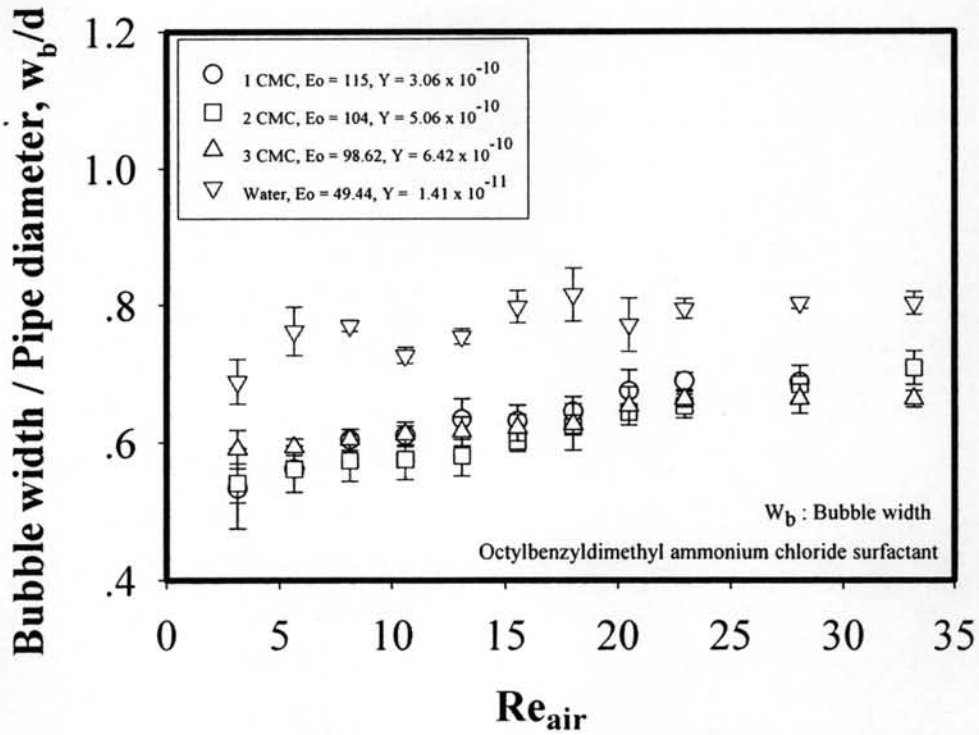
Bubble width / Pipe diameter, w_b/d
1.2
1.0
.8
.6
.4
1 CMC, Eo = 115, Y = 3.06 x 10^{-10}
2 CMC, Eo = 104, Y = 5.06 x 10^{-10}
3 CMC, Eo = 98.62, Y = 6.42 x 10^{-10}
Water, Eo = 49.44, Y = 1.41 x 10^{-11}
W_b : Bubble width
Octylbenzyldimethyl ammonium chloride surfactant
0 5 10 15 20 25 30 35
Re_{air}

(b)

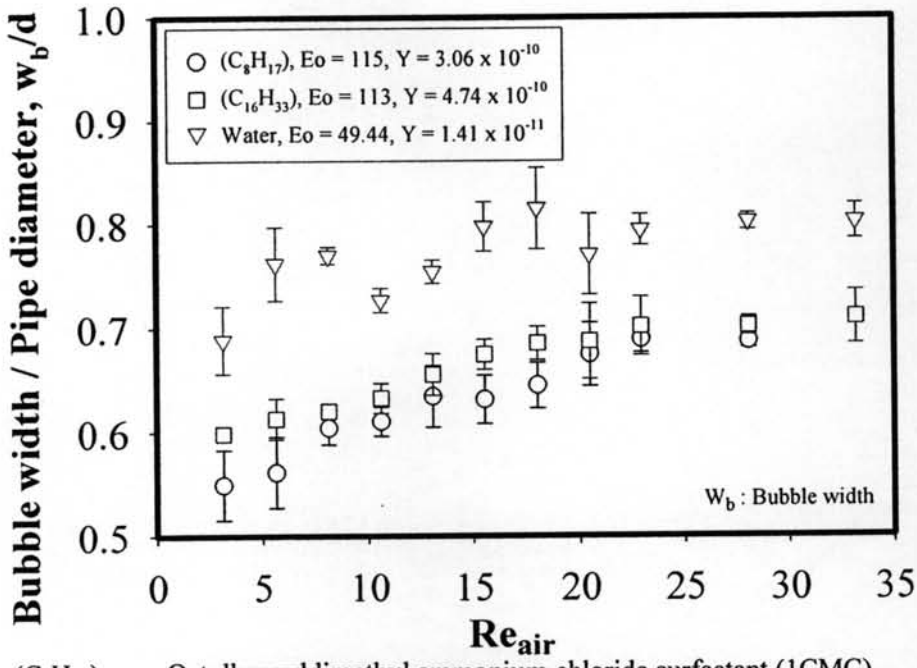

(C_8H_{17}) : Octylbenzyldimethyl ammonium chloride surfactant (1CMC)

$(C_{16}H_{33})$: Hexadecylbenzyldimethyl ammonium chloride surfactant (1CMC)

(c)

Figure 5 Bubble width vs. air Reynolds number: a) effect of Re_{liquid}= 0, 1001 and 2749, Eo = 115, Y = 3.06×10^{-10}; b) effect of concentration, Re_{liquid}= 2749, 2731, 2735 and 2740; c) effect of carbon tail length, Re_{liquid}= 2749, 2741 and 2740.

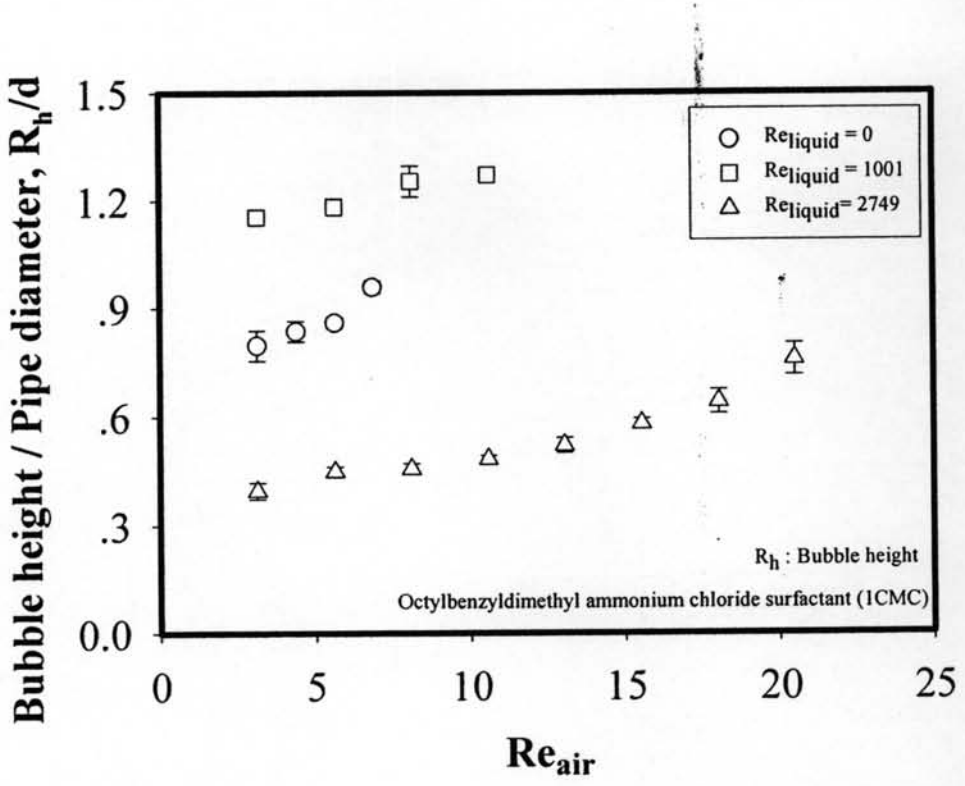
Bubble height / Pipe diameter, R_h/d
1.5
1.2
.9
.6
.3
0.0
0
5
10
15
20
25
Re_{air}
Re_{liquid} = 0
Re_{liquid} = 1001
Re_{liquid}= 2749
R_h : Bubble height
Octylbenzyldimethyl ammonium chloride surfactant (1CMC)

(a)

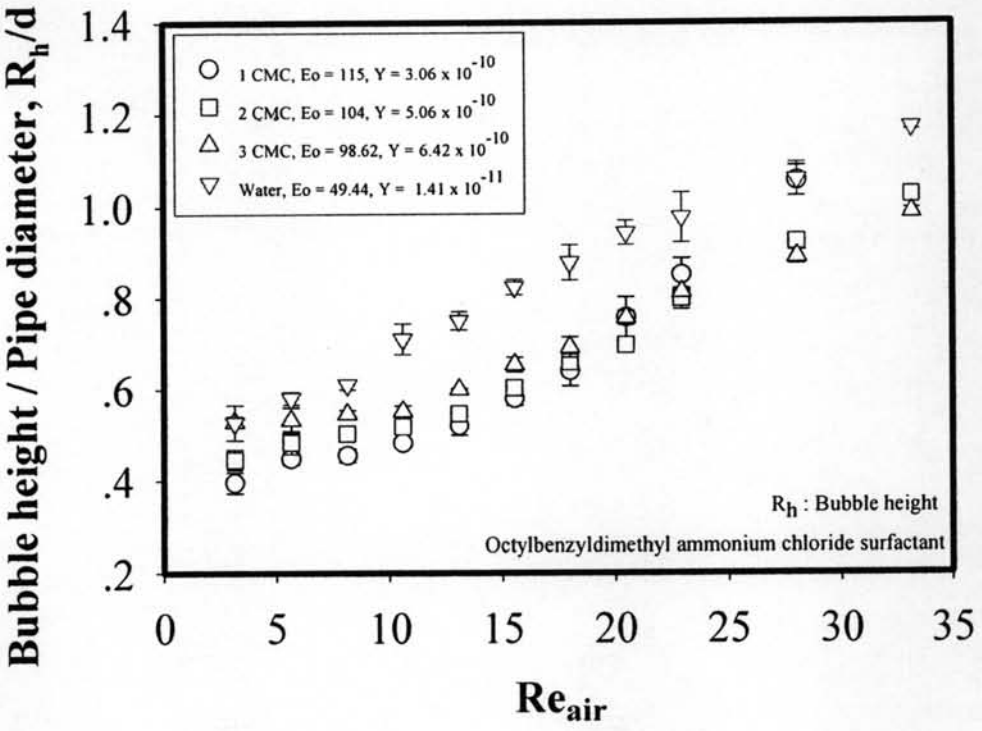
Bubble height / Pipe diameter, R_h/d
1.4
1.2
1.0
.8
.6
.4
.2
0
5
10
15
20
25
30
35
Re_{air}
1 CMC, Eo = 115, Y = 3.06 x 10^{-10}
2 CMC, Eo = 104, Y = 5.06 x 10^{-10}
3 CMC, Eo = 98.62, Y = 6.42 x 10^{-10}
Water, Eo = 49.44, Y = 1.41 x 10^{-11}
R_h : Bubble height
Octylbenzyldimethyl ammonium chloride surfactant

(b)

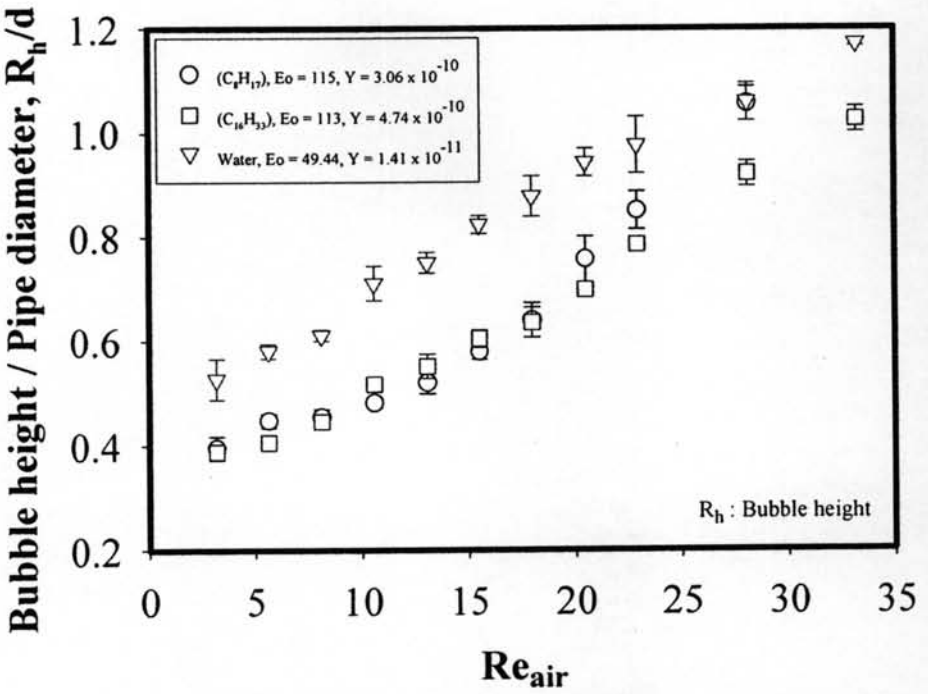

(C_8H_{17}) : Octylbenzyldimethyl ammonium chloride surfactant (1CMC)
$(C_{16}H_{33})$: Hexadecylbenzyldimethyl ammonium chloride surfactant (1CMC)

(c)

Figure 6 Bubble height vs. air Reynolds number: a) effect of Re_{liquid}= 0, 1001 and 2749, Eo = 115, Y = 3.06×10^{-10}; b) effect of concentration, Re_{liquid}= 2749, 2731, 2735 and 2740; c) effect of carbon tail length, Re_{liquid}= 2749, 2741 and 2740.

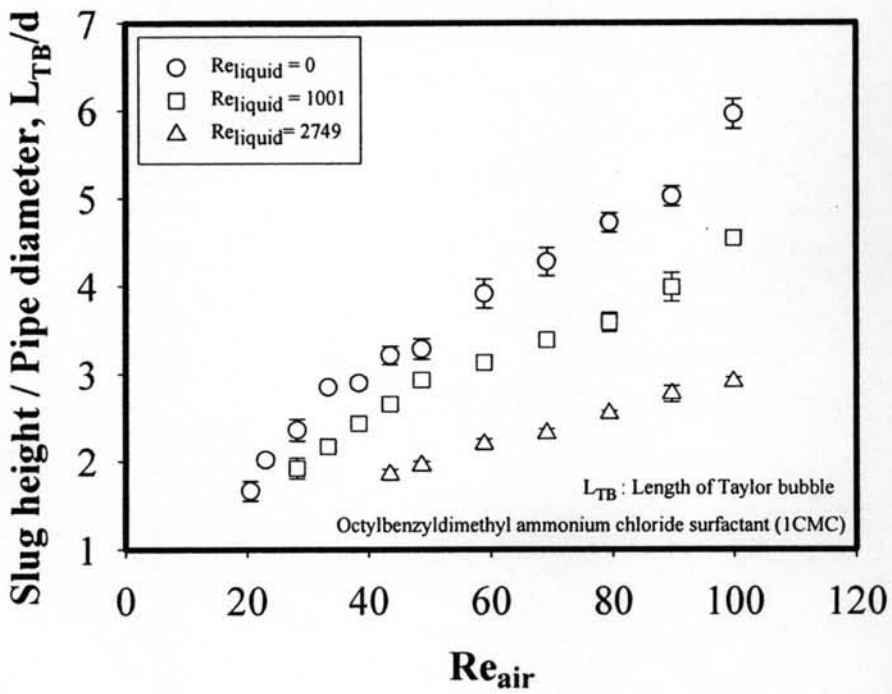
Slug height / Pipe diameter, L_{TB}/d
Re_{liquid} = 0
Re_{liquid} = 1001
Re_{liquid}= 2749
L_{TB} : Length of Taylor bubble
Octylbenzyldimethyl ammonium chloride surfactant (1CMC)
Re_{air}

(a)

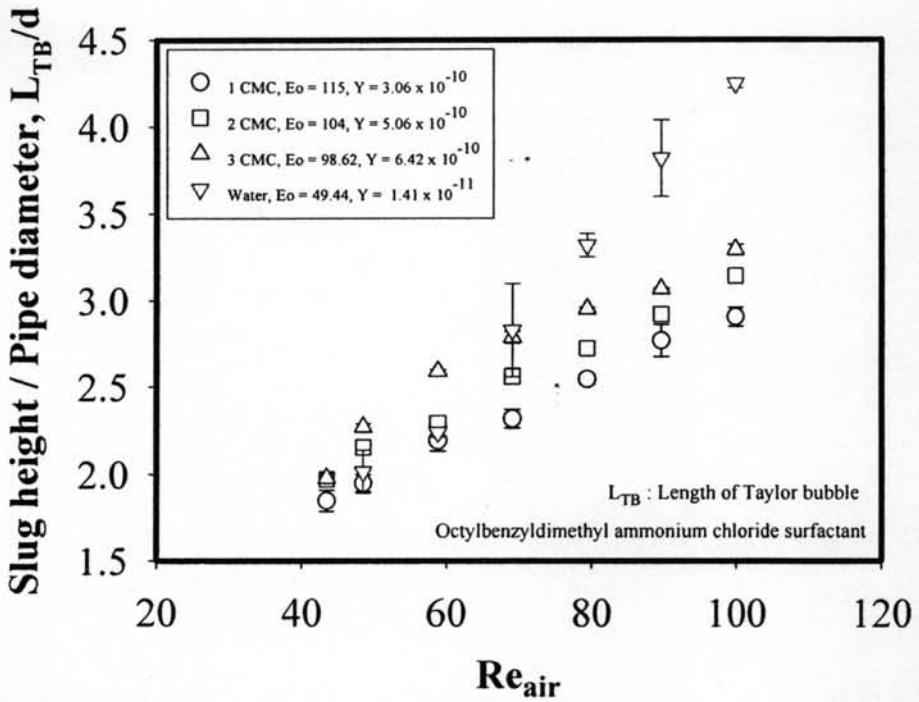
Slug height / Pipe diameter, L_{TB}/d
1 CMC, Eo = 115, Y = 3.06 x 10^{-10}
2 CMC, Eo = 104, Y = 5.06 x 10^{-10}
3 CMC, Eo = 98.62, Y = 6.42 x 10^{-10}
Water, Eo = 49.44, Y = 1.41 x 10^{-11}
L_{TB} : Length of Taylor bubble
Octylbenzyldimethyl ammonium chloride surfactant
Re_{air}

(b)

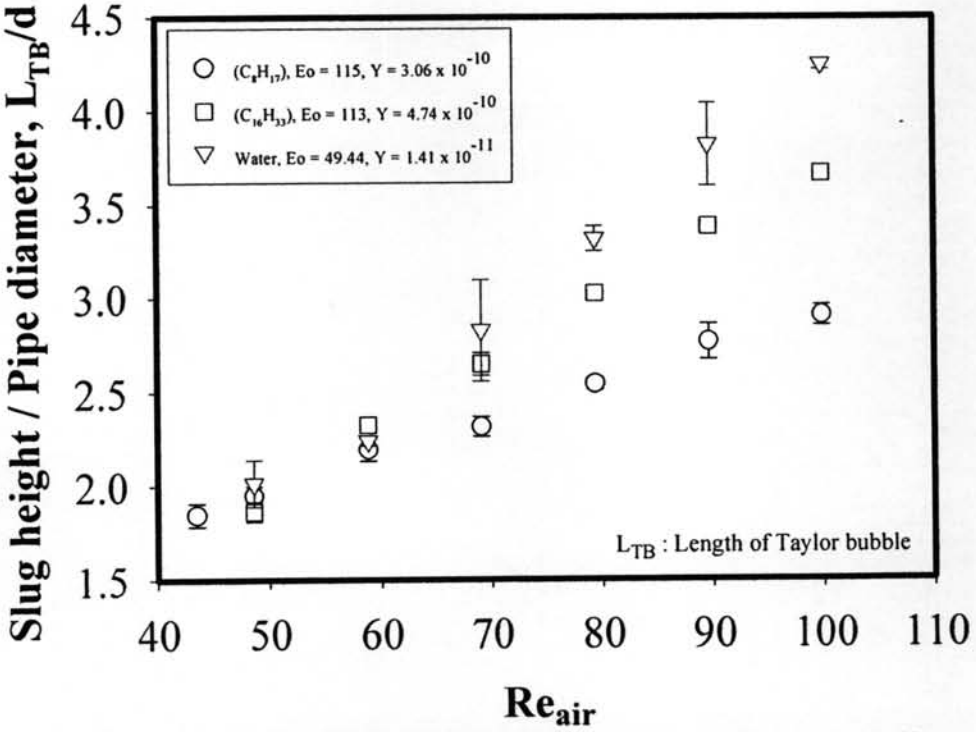

(C_8H_{17}) : Octylbenzyldimethyl ammonium chloride surfactant (1CMC)

$(C_{16}H_{33})$: Hexadecylbenzyldimethyl ammonium chloride surfactant (1CMC)

(c)

Figure 7 Slug height vs. air Reynolds number: a) effect of Re_{liquid}= 0, 1001 and 2749, Eo = 115, Y = 3.06×10^{-10}; b) effect of concentration, Re_{liquid}= 2749, 2731, 2735 and 2740; c) effect of carbon tail length, Re_{liquid}= 2749, 2741 and 2740.

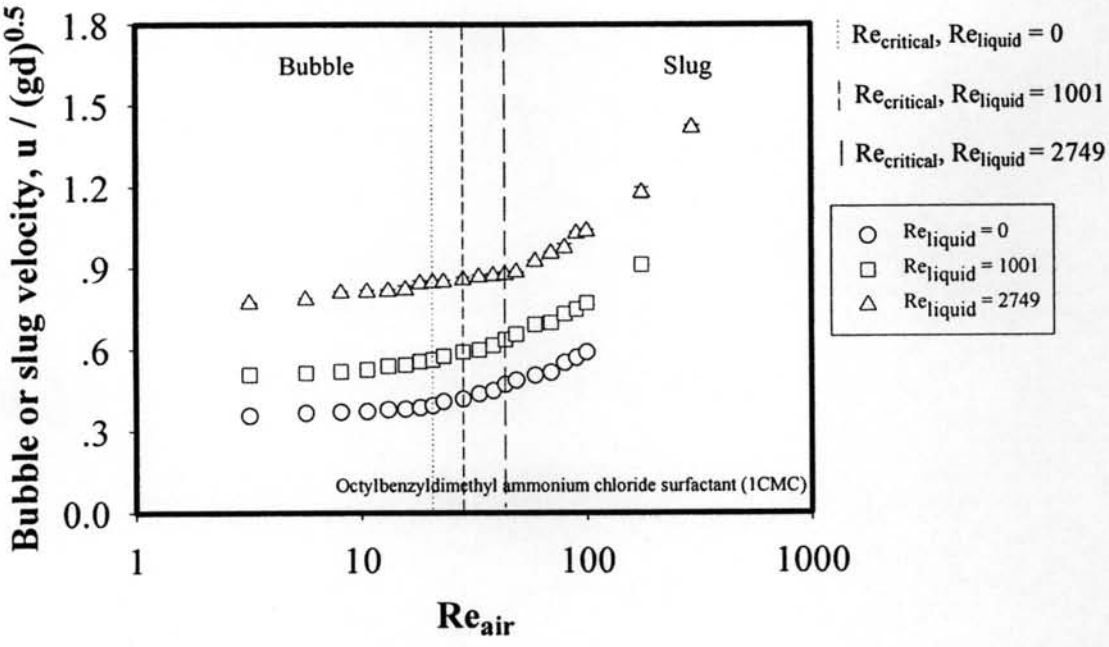
Bubble or slug velocity, u / (gd)^0.5
1.8
1.5
1.2
.9
.6
.3
0.0
Bubble
Slug
Octylbenzyldimethyl ammonium chloride surfactant (1CMC)
1
10
100
1000
Re_air
Re_critical, Re_liquid = 0
Re_critical, Re_liquid = 1001
Re_critical, Re_liquid = 2749
Re_liquid = 0
Re_liquid = 1001
Re_liquid = 2749

(a)

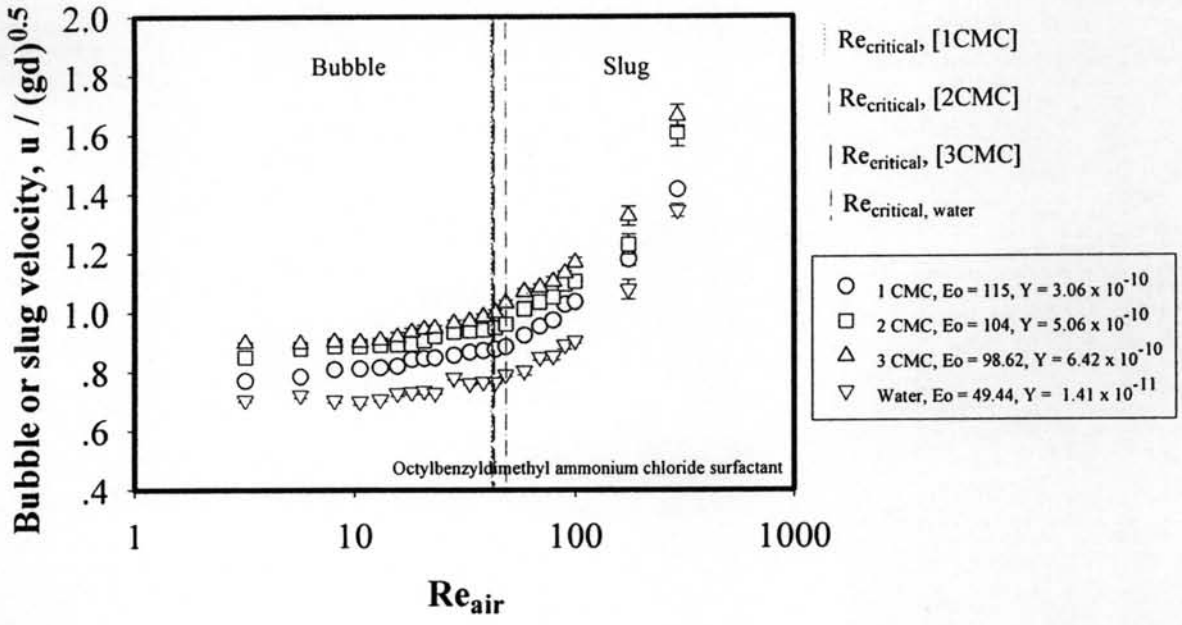
Bubble or slug velocity, u / (gd)^0.5
2.0
1.8
1.6
1.4
1.2
1.0
.8
.6
.4
Bubble
Slug
Octylbenzyldimethyl ammonium chloride surfactant
1
10
100
1000
Re_air
Re_critical, [1CMC]
Re_critical, [2CMC]
Re_critical, [3CMC]
Re_critical, water
1 CMC, Eo = 115, Y = 3.06 x 10^-10
2 CMC, Eo = 104, Y = 5.06 x 10^-10
3 CMC, Eo = 98.62, Y = 6.42 x 10^-10
Water, Eo = 49.44, Y = 1.41 x 10^-11

(b)

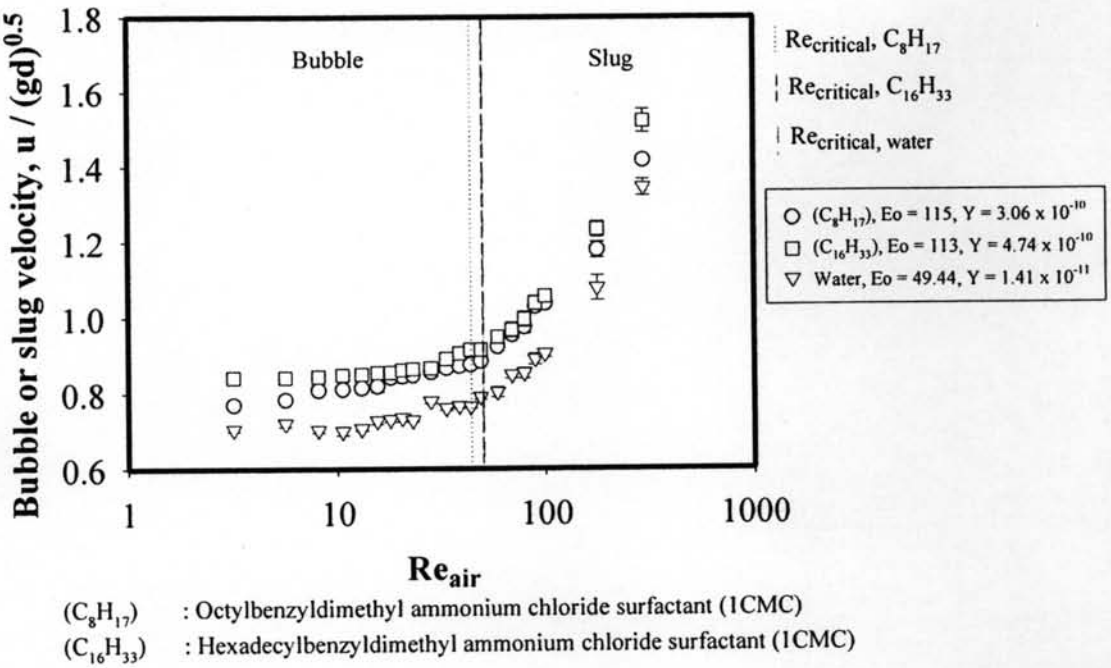

(C_8H_{17}) : Octylbenzyldimethyl ammonium chloride surfactant (1CMC)
($C_{16}H_{33}$) : Hexadecylbenzyldimethyl ammonium chloride surfactant (1CMC)

(c)

Figure 8 Bubble or slug velocity vs. air Reynolds number: a) effect of Re_{liquid}= 0, 1001 and 2749, Eo = 115, $Y = 3.06 \times 10^{-10}$; b) effect of concentration, Re_{liquid}= 2749, 2731, 2735 and 2740; c) effect of carbon tail length effect, Re_{liquid}= 2749, 2741 and 2740.